Chemical Engineering Journal 112 (2005) 131–135

Chemical Engineering Journal

www.elsevier.com/locate/cej

A knowledge-based pattern recognition approach for the prediction of bubble size distribution in Newtonian fluids at high pressure

C. Riverol [a,*], J. Cooney [b]

[a] Chemical Engineering Department, University of West Indies, St. Augustine, Trinidad, Trinidad and Tobago

[b] Process Engineering Department, Food Science Building, University College Cork, Cork, Ireland

Received 22 February 2005; received in revised form 11 July 2005; accepted 2 August 2005

Abstract

The knowledge-based pattern recognition (KE) approach provides a basis for classification of state of fluid systems. The new method determines bubble size distribution at high pressure that is very important for the brewery industry and other alcoholic beverages (champagne). Conforming to the principle of "decreasing precision with increasing intelligence", the KE approach has been applied to the determination of bubble size distribution. An important feature of these architectures is that they do not require global mathematical modeling of the system.

Keywords: Bubble size distribution; Pattern recognition; Fuzzy logic; Artificial intelligent

1. Introduction

It has been understood that the bubbling phenomena in the column has been one of the important factors in determining the levels of heat and mass transfer coefficients, thereby determining the performance of the bubble column reactors or contactors. However, little attention has been paid to the prediction of the bubble distribution mode at the distributor on the bubbling phenomena as well as transport phenomena in the pressurized bubble columns of a liquid medium. The resultant bubbling and complex flow behavior in multiphase flow systems have been successfully manipulated and interpreted by analyzing the fluctuations of their state variables such as pressure and temperature [1–3]. There are a wide variety of bubble measurement techniques that have been used in other areas [4] categorizes these techniques into three groups:

1. optical techniques (photography);
2. measurement of bubble volume (ultrasound/isokinetic sampling probes);
3. measurement of bubble penetration length along the axis where most movement takes place (bubble probes/optical fiber).

The simplest and commonest technique is however photography (this technique is used in this paper as comparative method). Photography has its own limitations, for example, images can only be obtained near the wall and also it is only a two-dimensional representation of a 3-D object. However, previously the major limitation of photography has been in the image processing. It is now feasible to take a large number of still images or a video and download them directly onto a PC. Here the images can be saved, discarded or analyzed, either manually or in certain cases automatically by the development of suitable imaging algorithms. Computer aided image analysis has been applied by many researchers, including those looking at bubble phenomenon. The present paper deals with the development of knowledge-based pattern recognition as alternative method for the prediction of the bubble size distribution. This approach provides a basis for classification based on structural states. The data obtained of such knowledge-based technique is compared with the optical technique (photography).

* Corresponding author. Tel.: +1 868 6622002; fax: +1 868 6624414.
E-mail address: criverol@eng.uwi.tt (C. Riverol).

1385-8947/$ – see front matter
doi:10.1016/j.cej.2005.08.002

Nomenclature

d	diameter
dc	credibility coefficient
FC	maximum value in the rule premise
g	gravity
u_f	mean
v	velocity
w	weight
x	distance between real value and center in the Gaussian membership function

Greek letters

μ	viscosity
μ_{ij}	membership function
ρ	density
σ_f	standard deviation

Isokinetic probes [5], involve sucking a small portion of dispersion from the vessel into a capillary where the bubbles form elongated slugs. In the case of beer haze, this method is compromised by continued growth of bubbles in the saturated solution [6]. Ultrasound requires a relatively dilute system and is compromised by re-scattering. In certain cases, ultrasound itself initiates bubble nucleation, which will affect the beer process [7].

Optical fiber probes [6] and electrical probes make use of differences in properties of the bubble and medium, to make local measurements of bubble penetration length and gas hold-up. These techniques have a minimum measurable bubble size and intrude into the vessel, which may later the gas–liquid flow pattern [4,6]. A fiber optic probe has been designed to measure solid holdup, bubble size, bubble rising velocity, particle rising velocity in both gas–solid and three-phase systems. The probe utilizes the difference in refractive index of gas and liquid to distinguish the gas phase from the liquid–solid suspension. The probe is of U-shape and there are variations in the tip designs for U-shaped probes to obtain maximum internal light reflection intensity for multiphase flow measurements. In the present probe, the fiber cladding in the tip portion is partially removed in such a manner that it yields the most distinctive signals for gas void detection. The output of the photomultiplier is interfaced with a computer data acquisition system, which samples the signal for four seconds at a frequency of 2000 Hz.

The probe is calibrated against the bubble rise velocity measured with a video camera. The probe is movable in the radial direction under high pressure conditions, so that the tip and the orifice can be precisely aligned. This feature also permits observation of the influence of the tip on the bubble flow or jetting phenomena. Based on visualization, the probe is found to impose negligible disturbances on the bubble formation process and the bubbling-jetting transition, although it would alter the trajectories of bubbles.

2. Classification of the structural state

The most important task in knowledge-based recognition procedure is the conversion of input process variables into features. The second is the translation of the classification logic expressed initially in natural linguistic form into a transparent recognition algorithm that yields from the structural variables membership to different classes. For the initial representation of the recognition algorithm, we consider a set of diagnosis rules that link the variables to the fluid system:

IF $\mu_{11}(\mathrm{x_j})$ and $\mu_{12}(x_j)$ ..., THEN (the process structural state belongs to State_1)
IF $\mu_{21}(x_j)$ and $\mu_{22}(x_j)$ ..., THEN (the process structural state belongs to State_2)
IF $\mu_{n1}(x_j)$ and $\mu_{n2}(x_j)$ ..., THEN (the process structural state belongs to State_n)

where $\mu_{ij}(x_j)$ is the fuzzy membership function and State_n is the subspace of the process. Two subspaces have been recognized:

- Bubble nucleation (State_1)
  The data at time zero could be used to estimate the number of bubbles produced during pouring, which in turn could be used to give a mean number of bubbles produced per second (dividing by the pouring time).
- Bubble growth (State_2)
  By comparing the data at consecutive time points, the evolution of the bubble size distribution could be observed. Local vertical velocities were estimated using Stoke's law $\left(v = \frac{gd^2\Delta\rho}{18\mu}\right)$ for each of the measured bubbles.

The states need to be transformed into an algorithm. It allows translation of the symbolic information into a numeric algorithm improving considerably their real response. For this, the following norm was adopted:

$$\begin{aligned} &\sum w_{ij}\mu_i = \mathrm{dc}_i \\ &\sum w_{ij} = \mathrm{CF}_i \end{aligned} \tag{1}$$

where w_{ij} are weight coefficients expressing the importance of the corresponding fuzzy membership and dc_i are functions formalizing the membership set (credibility). The norm implies that every fact contributes additively and with different weight to the overall certainty of the rule construction. An important step in the creation of the recognition procedure consists of determining the unknown weight coefficients w_{ij}. They can be estimated by linear regression using a training set composed of a time-series of the structural variables and the credibility coefficient (dc_i). The proper regression procedure was constructed using [5,6]. Its application to the rule system results in a set of equations as follows:

IF bubble velocity is low AND bubble diameter is low and pressure is zero, THEN bubble distribution is low (credibility 1.0);

Table 1
Membership fuzzy values

Variable	Segments	u_f	σ_f	Primary fuzzy sets
Bubble velocity (mm s^{-1})	[−2.0, 0.2]	−0.9	0.3	Low
	[0.2, 0.7]	0.03	0.3	Zero
	[0.1, 1.0]	0.5	0.2	High
Bubble diameter (mm)	[−1.0, 0.9]	−0.7	0.3	Low
	[0.2, 0.6]	0.1	0.3	Zero
	[0.4, 1.0]	0.55	0.2	High
Gas flow (L min^{-1})	[−1.0, 0.7]	−0.77	0.4	Low
	[0.2, 0.7]	0.05	0.3	Zero
	[0.5, 1.0]	0.43	0.3	High
Pressure (kPa)	[−1.0, 0.0]	−0.4	0.2	Low
	[−0.2, 0.7]	0.5	0.2	Zero
	[0.2, 1.0]	0.6	0.2	High
Liquid volume (L)	[−1.0, 0.1]	−0.6	0.3	Low
	[0.2, 0.6]	0.5	0.2	Zero
	[0.4, 1.0]	0.5	0.2	High
Bubble distribution (%)	[−1.0, 0.2]	−0.8	0.3	Low
	[0.2, 0.6]	0.05	0.3	Zero
	[0.4, 1.0]	0.5	0.2	High

IF bubble velocity is low AND bubble diameter is high and pressure is zero, THEN bubble distribution is high (credibility 1.0);
IF bubble velocity is low AND bubble diameter is zero and pressure is zero, THEN bubble distribution is zero (credibility 1.0);
IF bubble velocity is high AND bubble diameter is high and pressure is zero, THEN bubble distribution is high (credibility 1.0);
IF bubble velocity is low AND bubble diameter is zero and pressure is high, THEN bubble distribution is zero (credibility 1.0).

The rest of the combinations are considering with credibility 0.5. The partition of the continuous universe requires a priori knowledge of the input/output space. In Table 1 a functional definition expresses the membership function in a Gaussian shaped function. The functional definition can readily be adapted to a change in the universe. The functional definition was expressed as:

$$\mu_f = \exp\left[\frac{-(x-u_f)^2}{2\sigma_f^2}\right] \quad (2)$$

3. Experimental set up

The equipment is depicted in Fig. 1. A stainless steel high pressure column with an inner diameter of 9.96 cm and a height of 88.12 cm in the straight section was used. The column has an expanded section that serves to reduce the superficial liquid velocity before the liquid exits the column. Four pairs of quartz windows with polyethylene seals are installed on the front and rear sides of the column to allow the visualization of bubble characteristics. Each window is 10.0 mm in width and 83 mm height. A perforated plate with 96 pitches holes of 1.0 mm diameter is used as gas distributor. The high pressure is controlled using a back-pressure regulator installed at the outlet of the bubble column. The hydro-alcoholic solution is held within the pressure vessel and it was saturated to a pre-determined dissolved concentration of nitrogen (15%) and carbon dioxide (85%). The hydro-alcoholic solution was then ejected through the nozzle. The different variables are specified in Table 2. The bubble column has rectangular sides for avoid any distortion when viewing the bubbles.

Table 2
Variable specifications

Variable	Range
Pressure (kPa)	200–400
Gas flow (L min^{-1})	1.8–6.9
Alcohol content (g L^{-1})	95.9 (champagne approximately) and 53.1 (beer approximately)

4. Results and discussion

Figs. 2 and 3 show the bubble size distribution under various velocities at 200 kPa and the maximum stable bubble size at different pressures. In Fig. 2; the bubble size distributions are determined using the KE approach to 30 s intervals. The bubble diameter increases with the time and gas flow. The increase in median bubble diameter is as expected since the super-saturation. The breakage has been described by combining the collision frequency between the bubbles. The fact that KE approach neglects the physical processes affecting the probability of breakage, it is mathematically more favorable compared to many physical models. It produces zero probability for infinitely small daughter bubbles and the daughter bubbles equal to the size of mother bubble. Fig. 3 indicates that the maximum stable bubble size can be estimated by KE approach at pressures higher than 150 kPa, at lower pressures other models cited in the literature should be used. As the pressure increases, the gas density increases and the surface tension decreases, thus bubbles are less stable. The median bubble diameter was calculated using KE approach and compared using photography and the result is shown in Table 3.

As shown Table 3, the bubble formation rate increases when the gas flow increases, although the bubble formation rates decreases inversely with the pressure. In fact, Fig. 4 illustrates the effect of the velocity to bubble size. As for the bubble diameter, if the system is working at high pressure, the KE approach decreases its accuracy because the fluctuation of the liquid phase caused by bubbles is damped out as the pressure increases. Although the coalescence was estimated to both states in the KE approach using [7,8], the accuracy has not been improved. The velocity of each individual bubble in a bubble cloud is a combination of erratic small velocities.

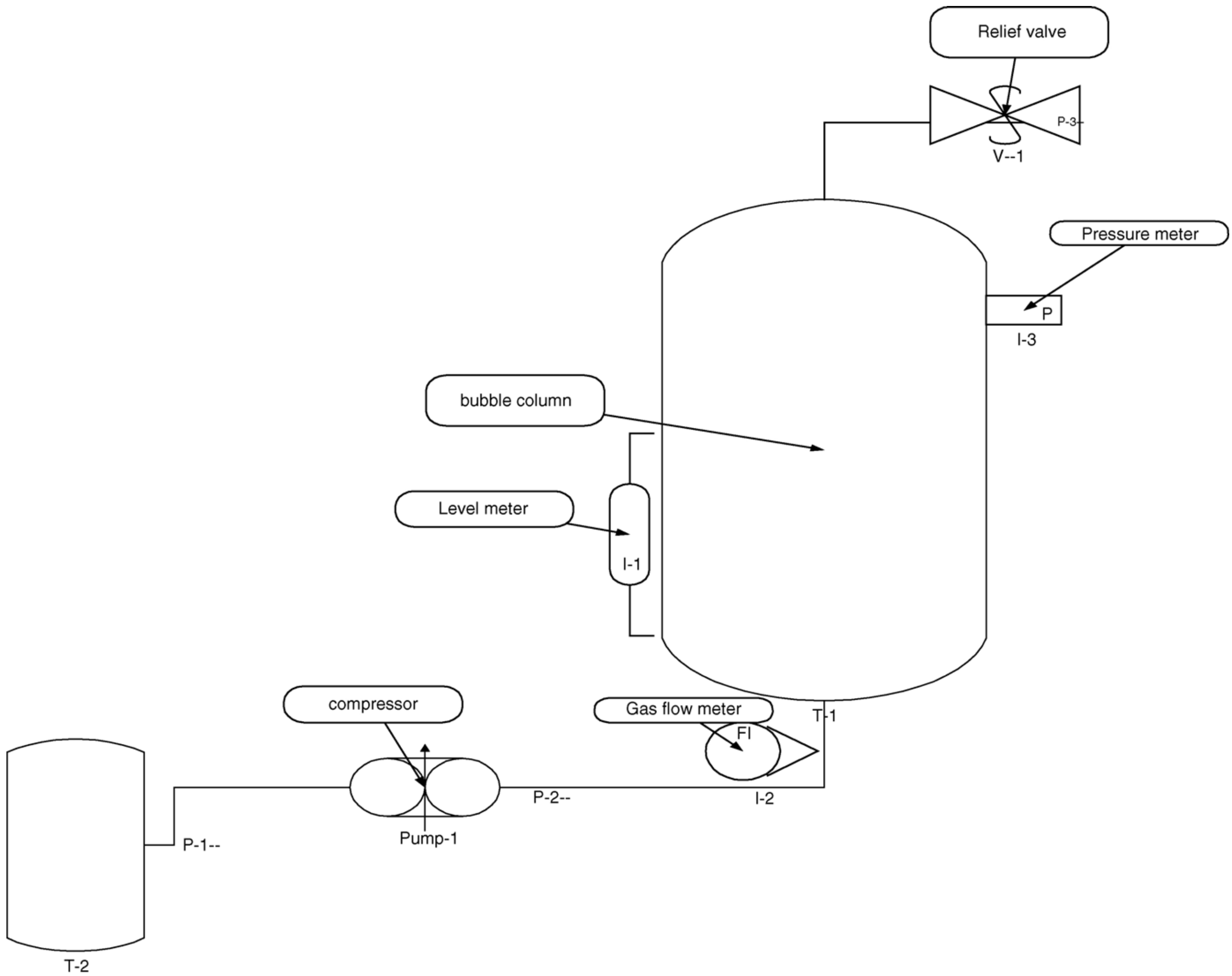

Fig. 1. Diagram of the bubble column.

The vertical velocity was calculated using Stoke's law; see Fig. 4 [9]. The vast majority of bubble velocities were below those defined by stokes law. It is likely that there is grouping among bubbles measured at different points of time suggest-

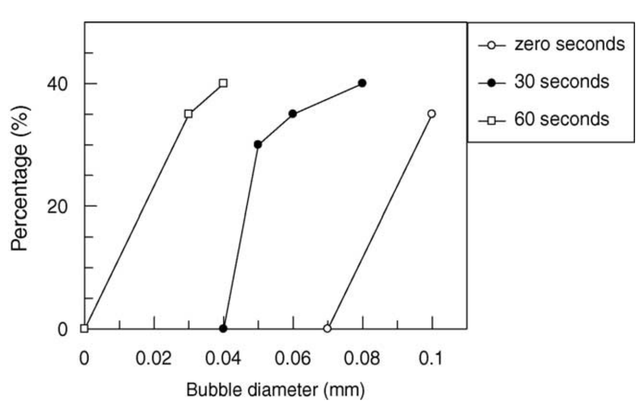

Fig. 2. Estimated bubble diameter at 200 kPa and 4.5 L min^{-1}.

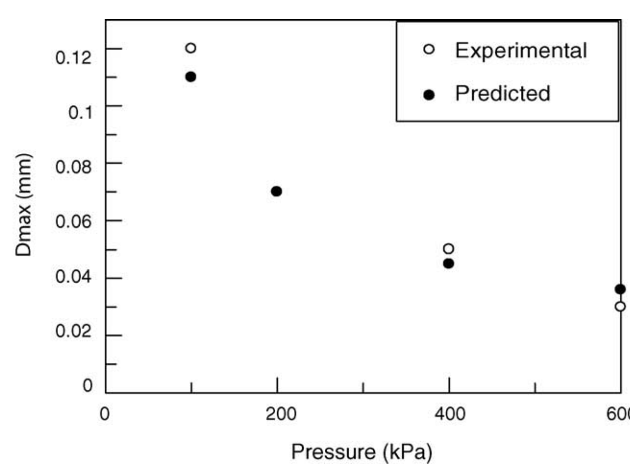

Fig. 3. Maximum stable diameter at 6.9 L min^{-1}: experimental data vs. predictions.

Table 3
Comparison of bubble diameter vs. pressure at different gas flows

Pressure: 200 kPa				
Gas flow (L min^{-1})	1.8	2.9	4.5	6.9
Bubble diameter (mm)	0.06	0.06	0.09	0.10
Bubble diameter (KE) (mm)	0.06	0.062	0.071	0.074
Bubble formation rate (bubble s^{-1})	90845	190400	590234	98342
Pressure: 300 kPa				
Gas flow (L min^{-1})	1.8	2.9	4.5	6.9
Bubble diameter (mm)	0.03	0.04	0.05	0.07
Bubble diameter (KE) (mm)	0.03	0.035	0.05	0.065
Bubble formation rate (bubble s^{-1})	90845	169490	440278	810921
Pressure: 400 kPa				
Gas flow (L min^{-1})	1.8	2.9	4.5	6.9
Bubble diameter (mm)	0.01	0.02	0.04	0.05
Bubble diameter (KE) (mm)	0.01	0.025	0.035	0.047
Bubble formation rate (bubble s^{-1})	70845	150300	34412	700200

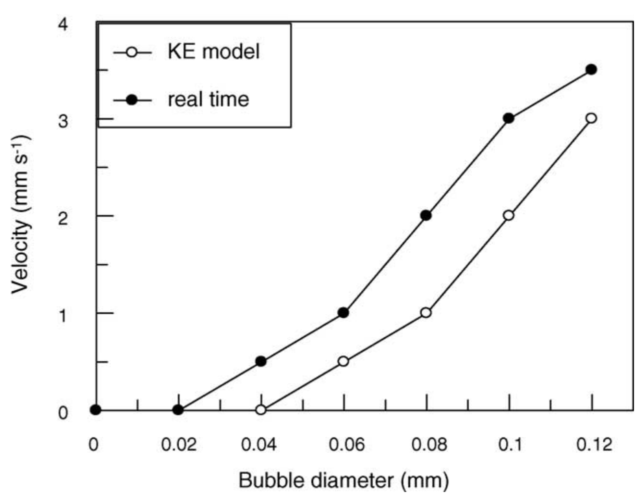

Fig. 4. Comparison real velocity vs. calculated velocity at 180 kPa.

ing that there is an external factor affecting all the bubble velocities. Moreover the effects of the coalescence are playing a part in the determination of the overall bubble velocity. It is worth nothing that the alcohol concentration does not affect the behavior of the bubbles; the above result was the same for both systems (beer and champagne).

5. Conclusion

Here we are shown one case where the knowledge-based approach can be useful in solving bubble size distribution problems resulting from the intrinsic variability of the system. The use and validation of the KE approach in the prediction of the mean bubble diameter indicated that this method was good enough. However, in uncertain environments, 100% success can be never be reached such is the case of the prediction of the vertical velocities as depicted Fig. 4. We consider the continuous accumulation of the knowledge concerning the underlying bubble behavior as our long-term task for improvement the accuracy and precision of the method.

References

[1] N.J. Hepworth, J. Varley, A. Hind, Characterizing gas bubble dispersions in beer, IChemE Trans. Part C Food Bioproducts Process. 79 (C1) (2001) 13–20.
[2] R. Lau, W. Peng, L.G. Velazquez-Vargas, G.Q. Yang, L.-S. Fan, Gas–liquid mass transfer in high-pressure bubble columns, Ind. Eng. Chem. Res. 43 (2004) 1302–1311, 5.
[3] T. Lin, K. Tsuchiya, L. Fan, Bubble flow characteristics in bubble columns at elevate pressure and temperature, AIChE J. 44 (1998) 44–54.
[4] R. Kikuchi, T. Yano, A. Tsutsumi, K. Yoshida, M. Puncochar, J. Drahos, Diagnosis of chaotic dynamics of bubble motion in a bubble column, Chem. Eng. Sci. 52 (1997) 3741–3745.
[5] W. Lu, L. Lin, Gas dispersion and bubble size distribution in dual impeller stirred vessels, J. Chin. Inst. Chem. Eng. 26 (2) (1995) 119–125.
[6] F. Takemura, A. Jabe, Gas dissolution process of spherical rising gas bubbles, Chem. Eng. Sci. 53 (15) (1998) 2691–2699.
[7] J. James, G. Suski, A survey of some implementations of knowledge-based systems for real-time control, in: Proceedings of the 27th IEEE Conference on Decision and Control, Austin, TX, 1988, pp. 580–585.
[8] K. Konstantinov, T. Yoshida, Physiological state control of fermentation processes, Biotechnol. Bioeng. (1989) 1145–1156.
[9] J. Joshi, Computational flow modeling and design of bubble column reactors, Chem. Eng. Sci. 56 (2001) 5893–5933.